



Journal of Advanced Research in Fluid Mechanics and Thermal Sciences

Journal homepage:
https://semarakilmu.com.my/journals/index.php/fluid_mechanics_thermal_sciences/index
ISSN: 2289-7879



Numerical Solution of Mixed Convection MHD Viscous Fluid Flow on Lower Stagnation Point of a Sliced Magnetic Sphere

Basuki Widodo^{1,*}, Adhi Surya Nugraha², Tri Rahayuningsih³

- ¹ Department of Mathematics, Faculty of Sciences and Data Analytics, Institut Teknologi Sepuluh Nopember, Kampus ITS Keputih Sukolilo, 60111, Surabaya, Indonesia
- ² Department of Mathematics Education, Faculty of Teacher Training and Education, Univesity of Sanata Dharma, Jalan Affandi, Mrican, Caturtunggal, Depok Sleman, 55281, Yogyakarta, Indonesia
- ³ Department of Agroindustrial Engineering, Faculty of Engineering, Wijaya Kusuma Surabaya University, Jalan Dukuh Kupang XXV no 54, 60225, Surabaya, Indonesia

ARTICLE INFO

Article history:

Received 17 October 2021

Received in revised form 29 March 2022

Accepted 3 April 2022

Available online 12 May 2022

Keywords:

Magnetohydrodynamic; magnetic sliced sphere; mix convection; viscous fluid; Keller-Box scheme

ABSTRACT

This paper considers mathematical modeling on mixed convection MHD viscous fluid flow on the lower stagnation point of a magnetic sliced sphere. The study began with transforming the governing equations which are in dimensional partial differential equations to non-dimensional ordinary differential equations by using the similarity variable. The resulting similarity equations are then solved by the Keller-Box scheme. The characteristics and effects of the Prandtl number, the sliced angle, the magnetic parameter, and the mixed convection parameter are analyzed and discussed.

1. Introduction

Nowadays, there have been many studies on MHD in various geometric shapes, such as the studies of Srinivasacharya and Reddy [1] on vertical plate, Jhumur and Bhattacharje [2] on L-shaped, Makinde and Aziz [3] on vertical plate, and Widodo *et al.*, [4] on sphere. In term of fluid types such as micropolar fluid, nanofluid, ferrofluid, and viscous fluid, the study of the MHD has been investigated by Alkasasbeh *et al.*, [5], Widodo and Ningtyas [6], Sajed *et al.*, [7], and Nugraha *et al.*, [8], respectively. In addition, in term of the conditions that influencing the MHD fluid flow can be seen in the papers that have been written by Widodo *et al.*, [9], Haq *et al.*, [10], and Prasad *et al.*, [11].

The importance thing of magnetic fluid flow had attracted researchers to study and explore its benefits and uses in the industrial sector, especially in convective flow and heat transfer processes. The studies of convective MHD flow and heat transfer on the stagnation point when the fluid flow

* Corresponding author.

E-mail address: b_widodo@matematika.its.ac.id

<https://doi.org/10.37934/arfmts.95.1.110120>

through the various geometry, such as sliced sphere and sphere, have been investigated by Widodo *et al.*, [12], Widodo *et al.*, [13], and Nursalim *et al.*, [14].

This paper considers the study of mixed convection viscous fluid magnetohydrodynamic flow on the lower stagnation point when the fluid through a magnetic sliced sphere. It therefore is interesting to study also the effect of the angle of the slice of the sphere.

1.1 Mathematical Modelling

Figure 1(a) and Figure 1(b) shows the physical model of the fluid flow and coordinate system, respectively. The mixed convection viscous fluid magnetohydrodynamic flow is assumed flowing in direction bottom to the top. Further, upstream temperature is denoted by T_∞ . Meanwhile, T_w is the surface temperature on the surface of the sliced magnetic sphere. In addition, there is also a sliced magnetic sphere with the slice angle θ_s located at the bottom of the sphere. The following figures are their illustration

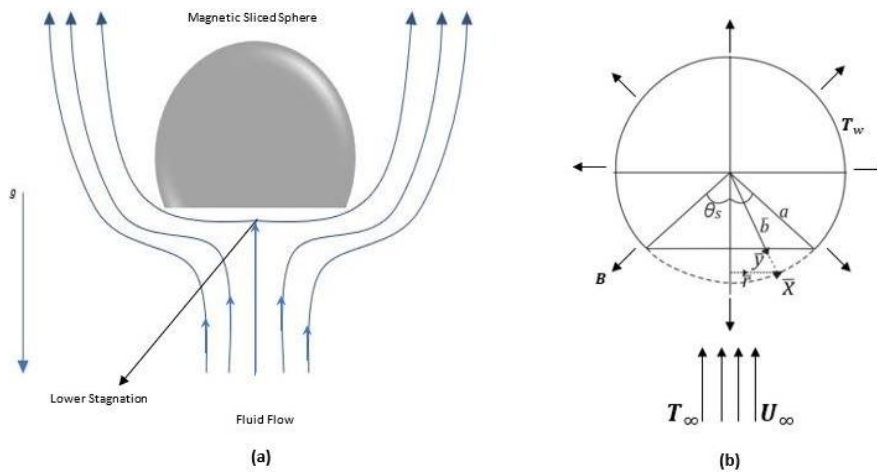


Fig. 1. (a) Physical Model of MHD fluid flow, (b) Sliced magnetic sphere and coordinate system

1.1.1 Dimensional governing equation

The 2-D dimensional governing equation further is developed from continuity, momentum, and energy equations as follows

Continuity equation

$$\frac{\partial(\bar{r}\bar{u})}{\partial\bar{x}} + \frac{\partial(\bar{r}\bar{v})}{\partial\bar{y}} = 0 \quad (1)$$

Momentum equation in-x direction

$$\rho \left(\frac{\partial\bar{u}}{\partial\bar{t}} + \bar{u} \frac{\partial\bar{u}}{\partial\bar{x}} + \bar{v} \frac{\partial\bar{u}}{\partial\bar{y}} \right) = -\frac{\partial\bar{p}}{\partial\bar{x}} + \mu \left(\frac{\partial^2\bar{u}}{\partial\bar{x}^2} + \frac{\partial^2\bar{u}}{\partial\bar{y}^2} \right) + \sigma(B_0 - b)^2\bar{u} - \rho\beta(\bar{T} - T_\infty)g_x \quad (2)$$

Momentum equation in-y direction

$$\rho \left(\frac{\partial\bar{v}}{\partial\bar{t}} + \bar{u} \frac{\partial\bar{v}}{\partial\bar{x}} + \bar{v} \frac{\partial\bar{v}}{\partial\bar{y}} \right) = -\frac{\partial\bar{p}}{\partial\bar{y}} + \mu \left(\frac{\partial^2\bar{v}}{\partial\bar{x}^2} + \frac{\partial^2\bar{v}}{\partial\bar{y}^2} \right) + \sigma(B_0 - b)^2\bar{v} - \rho\beta(\bar{T} - T_\infty)g_y \quad (3)$$

Energy equation

$$\rho C_p \left(\frac{\partial \bar{T}}{\partial \bar{t}} + \bar{u} \frac{\partial \bar{T}}{\partial \bar{x}} + \bar{v} \frac{\partial \bar{T}}{\partial \bar{y}} \right) = k \left(\frac{\partial^2 \bar{T}}{\partial \bar{x}^2} + \frac{\partial^2 \bar{T}}{\partial \bar{y}^2} \right) \quad (4)$$

with $g_{\bar{x}} = g \tan \left(\frac{x \cos \alpha}{\cos \theta_s} \right)$, and $g_y = \frac{g}{\cos \left(\frac{x \cos \alpha}{\cos \theta_s} \right)}$

subject to boundary conditions as follows

for $\bar{t} = 0$ then $\bar{u} = \bar{v} = 0, \bar{T} = T_\infty$ for any \bar{x}, \bar{y} ;

and for $\bar{t} > 0$ then $\bar{u} = \bar{v} = 0, \bar{T} = T_W$ at $\bar{y} = 0$, and $\bar{u} = \bar{u}_e(\bar{x}), \bar{T} = T_\infty$ at $\bar{y} \rightarrow \infty$.

where ρ is the fluid density, μ is fluid viscosity, g is gravity, β is coefficient of thermal expansion, C_p is specific heat, and k is heat flux. In addition, the value of r is defined as $\bar{r} = \bar{b} \sin \left(\frac{\bar{x}}{\bar{b}} \right)$ and the value of $\bar{u}_e = \frac{3}{2} U_\infty \sin \left(\frac{\bar{x}}{\bar{b}} \right)$, \bar{u}_e is a local free stream.

1.1.2 Non-dimensional governing equation

Further Eq. (1) to Eq. (4) to be transformed into non-dimensional governing equations by introducing dimensionless variables as follows

$$x = \frac{\bar{x}}{a}; y = Re \frac{\bar{y}}{a}; t = \frac{U_\infty \bar{t}}{a}; u = \frac{\bar{u}}{U_\infty}; v = Re \frac{\bar{v}}{U_\infty}; T = \frac{\bar{T} - T_\infty}{T_W - T_\infty}; p = \frac{\bar{p}}{\rho U_\infty^2};$$

By substituting these dimensionless variables into the dimensional equations of Eq. (1) to Eq. (4) can be written non-dimensional governing equations as follow

Continuity equation

$$\frac{\partial(ru)}{\partial x} + \frac{\partial(rv)}{\partial y} = 0 \quad (5)$$

Momentum equation in-x direction

$$\frac{\partial u}{\partial t} + u \frac{\partial u}{\partial x} + v \frac{\partial u}{\partial y} = -\frac{\partial p}{\partial x} + \frac{1}{Re} \frac{\partial^2 u}{\partial x^2} + \frac{\partial^2 u}{\partial y^2} + Mu + \alpha T \tan \left(\frac{x \cos \alpha}{\cos \theta_s} \right) \quad (6)$$

Momentum equation in-y direction

$$\frac{1}{Re} \left(\frac{\partial v}{\partial t} + u \frac{\partial v}{\partial x} + v \frac{\partial v}{\partial y} \right) = -\frac{\partial p}{\partial y} + \frac{1}{Re^2} \frac{\partial^2 v}{\partial x^2} + \frac{1}{Re} \frac{\partial^2 v}{\partial y^2} + \frac{M}{Re} v - \frac{\alpha T}{Re \frac{1}{2} \cos \left(\frac{x \cos \alpha}{\cos \theta_s} \right)} \quad (7)$$

Energy equation

$$\frac{\partial T}{\partial t} + u \frac{\partial T}{\partial x} + v \frac{\partial T}{\partial y} = \frac{1}{Re Pr} \frac{\partial^2 T}{\partial x^2} + \frac{1}{Pr} \frac{\partial^2 T}{\partial y^2} \quad (8)$$

where M is magnetic parameter, α is convection parameter, Gr is Grassof number and Pr is Prandtl number. Each of these parameters is defined as follows

$$M = \frac{\sigma(B_0 - b)^2 a}{\rho U_\infty};$$

$$\alpha = \frac{Gr}{Re^2};$$

$$Gr = \frac{g\beta(T_W - T_\infty)a^3}{\nu^2};$$

$$Pr = \frac{\nu\rho C_p}{c},$$

subject to boundary conditions as follows

for $t = 0$ then $u = v = 0, T = T_\infty$ for any x, y ;

and for $t > 0$ then $u = v = 0, T = T_W$ at $y = 0$, and $u = u_e(x), T = T_\infty$ at $y \rightarrow 0$.

Further, by using the boundary layer approximation, where the Reynold number $Re \rightarrow \infty$ which implies that $\frac{1}{Re} \rightarrow 0$, the Eq. (5) to Eq. (8) can each be expressed by

Continuity equation

$$\frac{\partial(ru)}{\partial x} + \frac{\partial(rv)}{\partial y} = 0 \tag{9}$$

Momentum equation

$$\frac{\partial u}{\partial t} + u \frac{\partial u}{\partial x} + v \frac{\partial u}{\partial y} = u_e \frac{\partial u_e}{\partial x} + \frac{\partial^2 u}{\partial y^2} + M(u - u_e) + \alpha T \tan\left(\frac{x \cos x}{\cos \theta_s}\right) \tag{10}$$

Energy equation

$$\frac{\partial T}{\partial t} + u \frac{\partial T}{\partial x} + v \frac{\partial T}{\partial y} = \frac{1}{Pr} \frac{\partial^2 T}{\partial y^2} \tag{11}$$

subject to boundary conditions as follows

for $t = 0$ then $u = v = 0, T = T_\infty$ for any x, y ;

and for $t > 0$ then $u = v = 0, T = T_W$ at $y = 0$, and $u = u_e(x), T = T_\infty$ at $y \rightarrow 0$.

1.1.3 Stream function

In the two-dimensional flow, the velocity in each $-x$ and $-y$ component can be expressed as stream function as follows

$$u = \frac{1}{r} \frac{\partial \psi}{\partial y}; \text{ and } v = -\frac{1}{r} \frac{\partial \psi}{\partial x} \tag{12}$$

Further, by substituting equation Eq. (12) into each equation Eq. (10) and Eq. (11), it is obtained,

Momentum equation

$$\frac{1}{r} \frac{\partial^2 \psi}{\partial t \partial y} + \frac{1}{r^2} \frac{\partial \psi}{\partial y} \frac{\partial^2 \psi}{\partial x \partial y} - \frac{1}{r^3} \frac{\partial r}{\partial x} \left(\frac{\partial \psi}{\partial y} \right)^2 - \frac{1}{r^2} \frac{\partial \psi}{\partial x} \frac{\partial^2 \psi}{\partial y^2} = u_e \frac{\partial u_e}{\partial x} + \frac{1}{r} \frac{\partial^3 \psi}{\partial y^3} + M \left(\frac{1}{r} \frac{\partial \psi}{\partial y} - u_e \right) + \alpha T \tan \left(\frac{x \cos x}{\cos \theta_s} \right) \quad (13)$$

Energy equation

$$\frac{\partial T}{\partial t} + \frac{1}{r} \frac{\partial \psi}{\partial y} \frac{\partial T}{\partial x} - \frac{1}{r} \frac{\partial \psi}{\partial x} \frac{\partial T}{\partial y} = \frac{1}{Pr} \frac{\partial^2 T}{\partial y^2} \quad (14)$$

with boundary conditions

$$t < 0; \psi = \frac{\partial \psi}{\partial y} = T = 0 \text{ for any } x, y;$$

$$t \geq 0; \psi = \frac{\partial \psi}{\partial y} = T = 1 \text{ at } y = 0;$$

$$\frac{\partial \psi}{\partial y} = u_e(x), T = 0 \text{ at } y \rightarrow \infty.$$

1.1.4 Similarity equation

By using similarity equations

for *small-time* ($t \leq t^*$) with t^* any value is

$$\psi = t^{\frac{1}{2}} u_e(x) r(x) f(x, \eta, t); T = s(x, \eta, t); \eta = \frac{y}{t^{\frac{1}{2}}} \quad (15)$$

for *large-time* ($t > t^*$) with t^* any value is

$$\psi = t^{\frac{1}{2}} u_e(x) r(x) F(x, Y, t); T = S(x, Y, t); Y = y \quad (16)$$

Further, by substituting Eq. (15) into Eq. (13) and Eq. (14), the following governing equations for small-time are obtained

Momentum equation

$$\frac{\partial^3 f}{\partial \eta^3} + \frac{\eta}{2} \frac{\partial^2 f}{\partial \eta^2} + t \frac{\partial u_e}{\partial x} \left(1 - \left(\frac{\partial f}{\partial \eta} \right)^2 + f \frac{\partial^2 f}{\partial \eta^2} \right) = t \frac{\partial^2 f}{\partial \eta \partial t} + t u_e \left(\frac{\partial f}{\partial \eta} \frac{\partial^2 f}{\partial \eta \partial x} - \frac{\partial f}{\partial x} \frac{\partial^2 f}{\partial \eta^2} - \frac{1}{r} \frac{\partial r}{\partial x} f \frac{\partial^2 f}{\partial \eta^2} \right) + M \left(1 - \frac{\partial f}{\partial \eta} \right) - \alpha t s \frac{\tan \left(\frac{x \cos x}{\cos \theta_s} \right)}{u_e} \quad (17)$$

Energy equation

$$\frac{\partial^2 s}{\partial \eta^2} + Pr \frac{\eta}{2} \frac{\partial s}{\partial \eta} + Pr t f \frac{\partial u_e}{\partial x} \frac{\partial s}{\partial \eta} = Pr t \left(\frac{\partial s}{\partial t} + u_e \left(\frac{\partial s}{\partial x} \frac{\partial f}{\partial \eta} - \frac{\partial f}{\partial x} \frac{\partial s}{\partial \eta} - \frac{f}{r} \frac{\partial r}{\partial x} \frac{\partial s}{\partial \eta} \right) \right) \quad (18)$$

And by substituting Eq. (16) into Eq. (13) and Eq. (14), the following governing equations for large time are obtained

Momentum equation

$$\frac{\partial^3 F}{\partial Y^3} + \frac{\partial u_e}{\partial x} \left(1 - \left(\frac{\partial F}{\partial Y} \right)^2 + F \frac{\partial^2 F}{\partial Y^2} \right) = \frac{\partial^2 F}{\partial Y \partial t} + u_e \left(\frac{\partial F}{\partial Y} \frac{\partial^2 F}{\partial Y \partial x} - \frac{\partial F}{\partial x} \frac{\partial^2 F}{\partial Y^2} - \frac{1}{r} \frac{\partial r}{\partial x} F \frac{\partial^2 F}{\partial Y^2} \right) + M \left(1 - \frac{\partial F}{\partial Y} \right) - \alpha S \frac{\tan\left(\frac{x \cos \theta_s}{\cos \theta_s}\right)}{u_e} \quad (19)$$

Energy equation

$$\frac{\partial^2 S}{\partial Y^2} + Pr \frac{\partial u_e}{\partial x} F \frac{\partial S}{\partial Y} = Pr \left(\frac{\partial S}{\partial t} + u_e \left(\frac{\partial S}{\partial x} \frac{\partial F}{\partial Y} - \frac{\partial F}{\partial x} \frac{\partial S}{\partial Y} - \frac{F}{r} \frac{\partial r}{\partial x} \frac{\partial S}{\partial Y} \right) \right) \quad (20)$$

Especially at lower stagnation point (when $x = 0$), the governing equations for *small-time* are reduced to:

Momentum equation

$$\frac{\partial^3 f}{\partial \eta^3} + \frac{\eta}{2} \frac{\partial^2 f}{\partial \eta^2} + \frac{3t}{2 \cos \theta_s} \left(1 - \left(\frac{\partial f}{\partial \eta} \right)^2 + f \frac{\partial^2 f}{\partial \eta^2} \right) = t \frac{\partial^2 f}{\partial t \partial \eta} + Mt \left(1 - \frac{\partial f}{\partial \eta} \right) - \frac{2}{3} \alpha t s \quad (21)$$

Energy equation

$$\frac{\partial^2 s}{\partial \eta^2} + Pr \frac{\eta}{2} \frac{\partial s}{\partial \eta} + Pr t f \frac{3}{2 \cos \theta_s} \frac{\partial s}{\partial \eta} = Pr t \frac{\partial s}{\partial t} \quad (22)$$

with boundary conditions

$$t = 0 : f = \frac{\partial f}{\partial \eta} = s = 0 \text{ for any } x, \eta$$

$$t > 0 : f = \frac{\partial f}{\partial \eta} = 0, s = 1 \text{ at } \eta = 0$$

$$\frac{\partial f}{\partial \eta} = 1, s = 0 \text{ at } \eta \rightarrow \infty$$

whereas for the large time, at stagnation point (when $x = 0$), the equations are reduced to

Momentum equation

$$\frac{\partial^3 F}{\partial Y^3} + \frac{3t}{2 \cos \theta_s} \left(1 - \left(\frac{\partial F}{\partial Y} \right)^2 + F \frac{\partial^2 F}{\partial Y^2} \right) = \frac{\partial^2 F}{\partial t \partial Y} + M \left(1 - \frac{\partial F}{\partial Y} \right) - \frac{2}{3} \alpha S \quad (23)$$

Energy equation

$$\frac{\partial^2 S}{\partial Y^2} + Pr \frac{3}{2 \cos \theta_s} F \frac{\partial S}{\partial Y} = Pr \frac{\partial S}{\partial t} \quad (24)$$

with the boundary conditions

$$F = \frac{\partial F}{\partial Y} = 0, S = 1 \text{ at } Y = 0; \frac{\partial F}{\partial Y} = 1, S = 0 \text{ at } Y \rightarrow \infty$$

2. Methodology

The problems of mixed convection MHD viscous fluid flow on the lower stagnation point of a magnetic sliced sphere further is solved numerically using the Keller-Box method the same as that used in the study conducted by Al-Shibani *et al.*, [15], Osman and Langlands [16], and Habib *et al.*, [17]. There are four steps as follows

- i. Reducing the transformed equations to a first-order system.
- ii. Write the difference equations using central differences.
- iii. Taking Linearization of the resulting algebraic equations by Newton method and writing them into matrix-vector form.
- iv. Solving the linear system by block tridiagonal eliminations technique.

3. Results and Discussions

The effects of various parameters, such as Prandtl number (Pr), magnetic parameter (M), sliced angle parameter (θ_s), and mixed convection parameter (α) are applied to investigate velocity and temperature on the lower stagnation point. Further, the problem is numerically solved by the finite difference method using the Keller-Box scheme. The computer programming is developed using MATLAB.

Table 1
Magnetic parameter values based on sphere material

Magnetic sphere	ρ	σ	M
Iron	7.87×10^3	1.04×10^7	1.3
Cobalt	8.86×10^3	1.6×10^7	1.8
Steel	7.75×10^3	1.61×10^7	2.0
Zinc	7.14×10^3	1.68×10^7	2.3

The current results are further compared with the results obtained from the study of Widodo *et al.*, [13] where $M = 1.3, \alpha = 1, Pr = 0.7$, and $\theta_s = 0$. The difference between the current study and Widodo *et al.*, [13] are that in the current study the sphere has no effect on the slice angle, and for Widodo *et al.*, [13] problem is solved by using an implicit finite difference method. Figure 2 shows comparison of present and Widodo *et al.*, [13] results.

Figure 2 shows that Figure 2(a) the velocity and Figure 2(b) the temperature of the present study and Widodo *et al.*, [13] are coincided. This coincidence means that the results of the current study are confirmed. The numerical results of the current study further can be used for other parameters and variables that are appropriate to the problem in the current study.

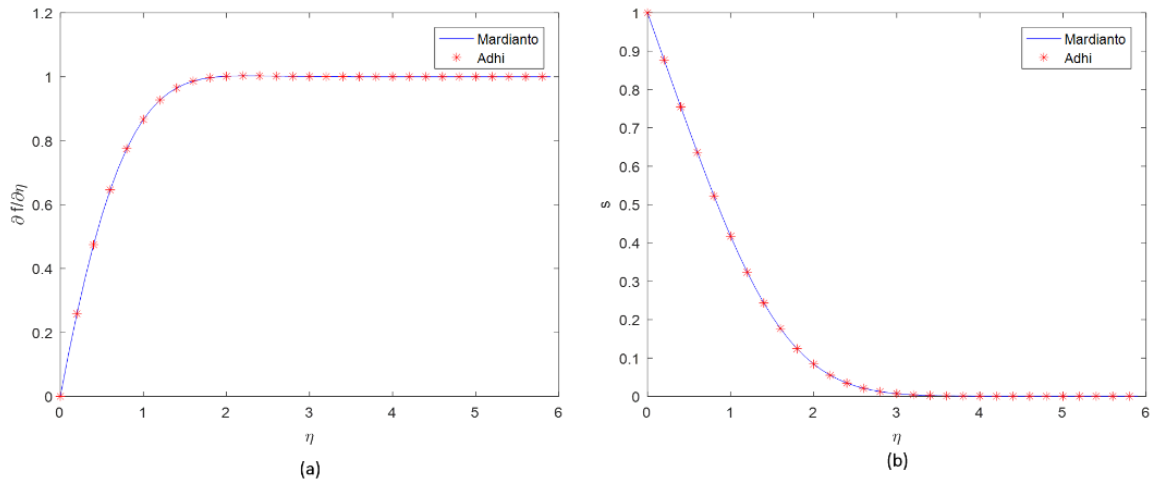


Fig. 2. (a) Velocity and (b) Temperature

3.1 Variations in Magnetic Parameter

Figure 3 shows numerical results with variations in magnetic parameters. The variation of the magnetic parameters used in this numerical calculation is as shown in Table 1 and the fixed value of the other parameters used are $\alpha = 1$, $Pr = 0.7$, and $\theta_s = 30^\circ$.

Figure 3(a) illustrates that an increase in the magnetic parameter causes a decrease in the fluid velocity. This happens because the increase in the magnetic parameter causes an increase in the Lorentz force which holds the fluid close to the spherical surface. So the fluid velocity is reduced. Figure 3(b) shows that an increase in the magnetic parameter causes an increase in the fluid temperature. This is due to the large number of fluid particles that are retained by the Lorentz force so that the distance between the particles is getting closer.

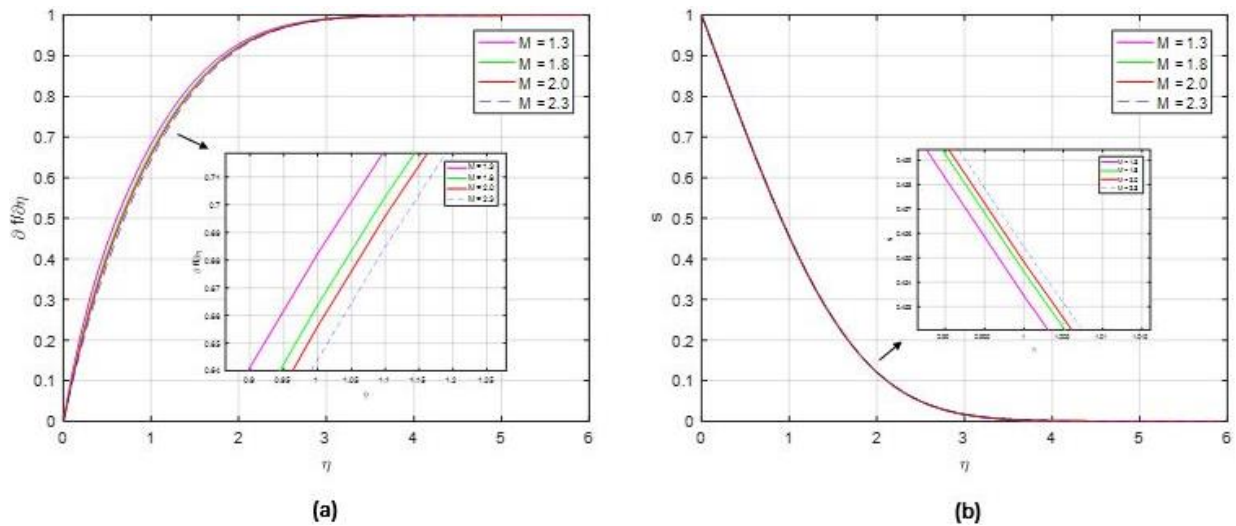


Fig. 3. (a) velocity and (b) temperature for various magnetic parameters

This causes the opportunity for friction between particles to become more frequent, causing the internal temperature to increase.

3.2 Variations in Convection Parameter

The variation of convection parameters used in Figure 4 are $\alpha = 1, 2, 3,$ and $4,$ when the fixed value of other parameters are $M=1, Pr=0.7,$ and $\theta_s = 45^\circ.$

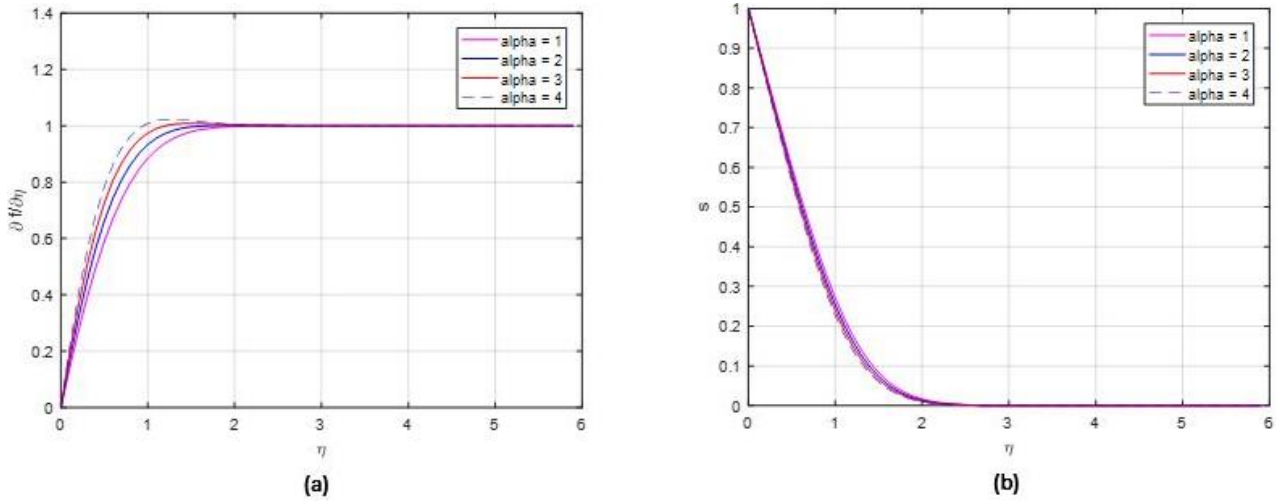


Fig. 4. (a) velocity and (b) temperature for various convection

Figure 4(a) shows that the fluid velocity increases when the convection parameter is increased in value. This occurs because of the additional energy in the fluid flow caused by the external force exerted on it. Meanwhile, Figure 4(b) shows that the fluid temperature decreases when the convection parameter value is increased. This happens because the fluid particle force is dominant over the Lorentz force so that there is no increase in the internal temperature of the fluid due to friction between fluids or repulsive forces that arise in the fluid flow.

3.3 Variations in Prandtl Number Parameter

The variation of the Prandtl number parameter used in Figure 5 is $Pr = 0.7$ (Gas), 1 (Brine), 7 (Water), and 100 (Oil), with fixed values for other parameters are $M=2, \alpha=2,$ and $\theta_s = 45^\circ.$

Figure 5(a) shows that the fluid velocity decreases as the value of the Prandtl number is increased. This happens because increasing the Prandtl number results in an increase in the density of the fluid.

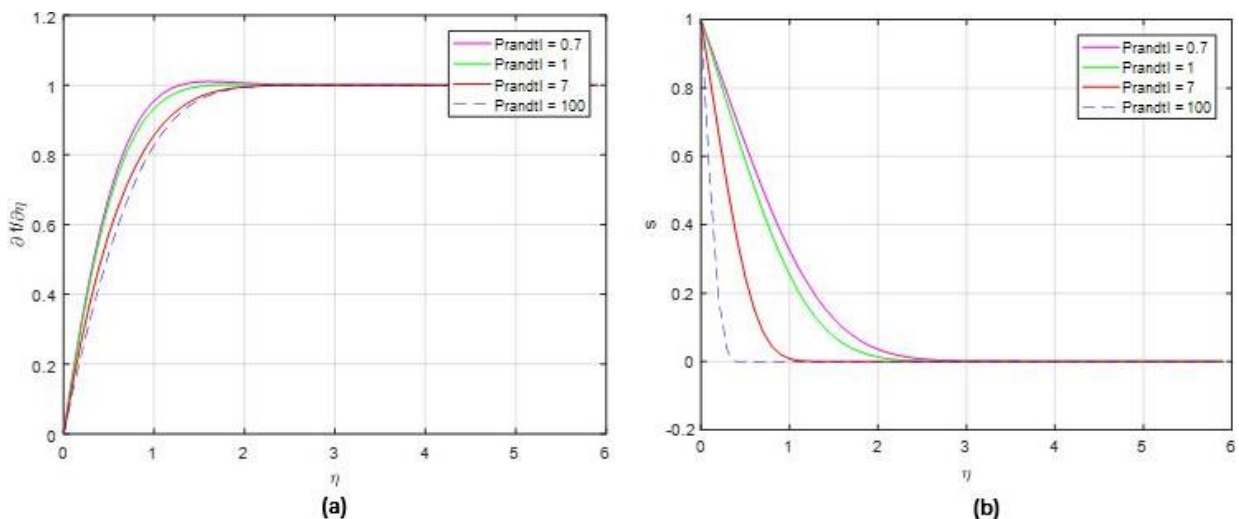


Fig. 5. (a) velocity and (b) temperature for various Prandtl number

This causes the fluid particles to flow more slowly. Figure 5(b) shows that the temperature of the fluid decreases when the value of the Prandtl number is increased. This happens because increasing the value of the Prandtl number has an impact on decreasing the thermal conductivity so that the heat distribution in the fluid decreases slowly and causes the temperature of the fluid to decrease.

3.4 Variations in The Angle of Slice of The Sphere

Variations of the spherical slice parameters θ_s used in Figure 6 are $\theta_s = 15, 30, 45, 60, 65, 70,$ and 85 , the fixed values for other parameters are $M=2, \beta=1,$ and $Pr=0.7$.

Figure 6(a) shows that the velocity of the fluid increases with the increase in the angle of slice on the sphere. This happens because the lower surface of the sliced ball gets wider which results in reduced friction between the fluid and the surface so that its velocity increases. Figure 6(b) shows that the temperature of the fluid decreases with increasing the angle of slice on the sphere. This happens because the greater the angle of slice on the sphere causes the surface under the sphere to become wider, which has an impact on the temperature at the bottom of the sphere decreasing faster so that the fluid temperature decreases.

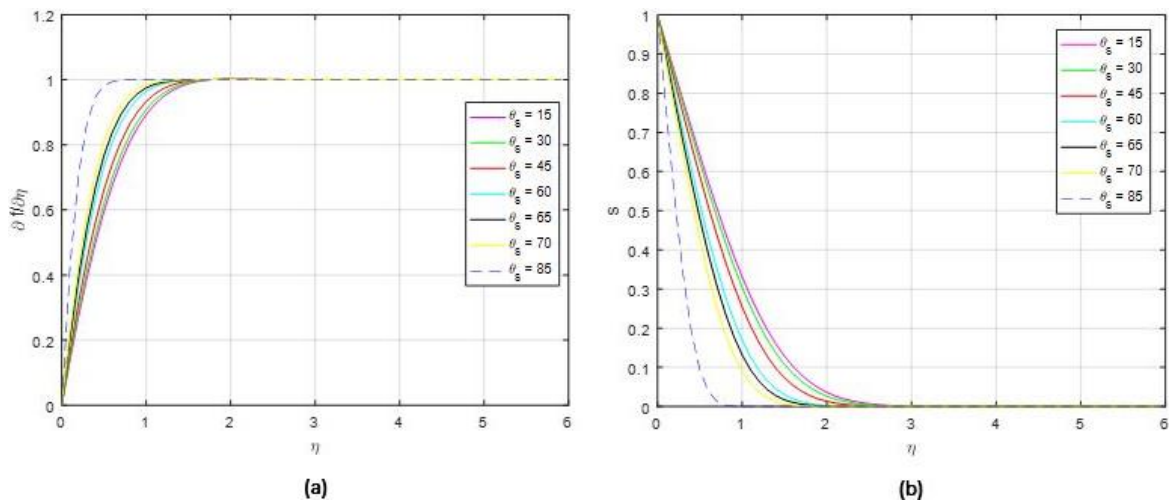


Fig. 6. (a) velocity and (b) temperature for various slicing

4. Conclusion

A study of the numerical solution of the mixed convection viscous fluid flow problem at the lower stagnation point of the magnetic sphere wedge has been carried out. The result is that

- i. If the value of the magnetic parameter is increased, the fluid velocity decreases and the fluid temperature increases,
- ii. If the convection parameter value is increased, the fluid velocity increases, but the fluid temperature decreases,
- iii. If the Prandtl number is increased, the velocity and temperature of the fluid decrease,
- iv. If the angle of the wedge of the lower sphere is increased, the velocity of the fluid increases but the temperature of the fluid decreases.

Acknowledgment

This research was supported by funding from the Directorate of Research and Community Development (DRPM) of the Sepuluh Nopember Institute of Technology Surabaya, East Java,

Indonesia. Therefore, we are very grateful to DRPM-ITS for giving us the opportunity to publish this paper in the Journal of Advanced Research in Fluid Mechanics and Thermal Sciences.

References

- [1] Srinivasacharya, D., and G. Swamy Reddy. "Mixed convection on a vertical plate in a power-law fluid saturated porous medium with cross diffusion effects." *Procedia Engineering* 127 (2015): 591-597. <https://doi.org/10.1016/j.proeng.2015.11.349>
- [2] Jhumur, Nandita Chakrabarty, and Anuruddha Bhattacharjee. "Unsteady MHD mixed convection inside L-shaped enclosure in the presence of ferrofluid (Fe_3O_4)." *Procedia Engineering* 194 (2017): 494-501. <https://doi.org/10.1016/j.proeng.2017.08.176>
- [3] Makinde, Oluwole Daniel, and A. Aziz. "MHD mixed convection from a vertical plate embedded in a porous medium with a convective boundary condition." *International Journal of Thermal Sciences* 49, no. 9 (2010): 1813-1820. <https://doi.org/10.1016/j.ijthermalsci.2010.05.015>
- [4] Widodo, Basuki, Adhi Surya Nugraha, and Muhammad Thahiruddin. "Numerical Solution of Unsteady Al_2O_3 -Water Nanofluid Flow Past A Magnetic Porous Sliced Sphere." In *Journal of Physics: Conference Series*, vol. 1490, no. 1, p. 012070. IOP Publishing, 2020. <https://doi.org/10.1088/1742-6596/1490/1/012070>
- [5] Alkawasbeh, Hamzeh T., Mohammed Z. Swalmeh, Abid Hussanan, and Mustafa Mamat. "Effects of mixed convection on methanol and kerosene oil based micropolar nanofluid containing oxide nanoparticles." *CFD Letters* 11, no. 1 (2019): 55-68.
- [6] Widodo, Basuki, and Rita Ayu Ningtyas. "The Unsteady Micropolar Fluid Flow Past A Sliced Sphere." *International Journal of Chemical Concepts* 3, no. 2 (2017): 218-224.
- [7] Sajid, M., S. A. Iqbal, M. Naveed, and Z. Abbas. "Joule heating and magnetohydrodynamic effects on ferrofluid (Fe_3O_4) flow in a semi-porous curved channel." *Journal of Molecular Liquids* 222 (2016): 1115-1120. <https://doi.org/10.1016/j.molliq.2016.08.001>
- [8] Nugraha, A. S., B. Widodo, and C. Imron. "Unsteady magnetohydrodynamics of viscous fluid past a magnetic sliced sphere." In *AIP Conference Proceedings*, vol. 2242, no. 1, p. 030007. AIP Publishing LLC, 2020. <https://doi.org/10.1063/5.0007930>
- [9] Widodo, Basuki, Indira Anggriani, Dwi Ariyani Khalimah, Firdha Dwi Shafarina Zainal, and Chairul Imron. "Unsteady Boundary Layer Magnetohydrodynamics in Micropolar Fluid Past A Sphere." *Far East Journal of Mathematical Sciences (FJMS)* 100, no. 2 (2016): 291-299. <https://doi.org/10.17654/MS100020291>
- [10] Haq, Sami Ul, Muhammad Atif Khan, and Nehad Ali Shah. "Analysis of magnetohydrodynamic flow of a fractional viscous fluid through a porous medium." *Chinese Journal of Physics* 56, no. 1 (2018): 261-269. <https://doi.org/10.1016/j.cjph.2017.12.020>
- [11] Prasad, V. Ramachandra, B. A. B. O. Vasu, O. Anwar Bég, and Rana D. Parshad. "Thermal radiation effects on magnetohydrodynamic free convection heat and mass transfer from a sphere in a variable porosity regime." *Communications in Nonlinear Science and Numerical Simulation* 17, no. 2 (2012): 654-671. <https://doi.org/10.1016/j.cnsns.2011.04.033>
- [12] Widodo, B., D. A. Khalimah, F. D. S. Zainal, and C. Imron. "The Effect of Prandtl Number and Magnetic Parameters on Unsteady Magnetohydrodynamic Forced Convection Boundary Layer Flow of A Viscous Fluid Past A Sphere." *International Journal of Advances in Science Engineering and Technology* 4, no. 1 (2016): 75-78.
- [13] Widodo, Basuki, Lutfi Mardianto, and Dieky Adzkiya. "Numerical investigation on magnetohydrodynamics mixed convection flow past a magnetic sphere." In *Journal of Physics: Conference Series*, vol. 1153, no. 1, p. 012059. IOP Publishing, 2019. <https://doi.org/10.1088/1742-6596/1153/1/012059>
- [14] Nursalim, Rahmat, Basuki Widodo, and Chairul Imron. "Magnetohydrodynamics of unsteady viscous fluid on boundary layer past a sliced sphere." In *Journal of Physics: Conference Series*, vol. 893, no. 1, p. 012044. IOP Publishing, 2017. <https://doi.org/10.1088/1742-6596/893/1/012044>
- [15] Al-Shibani, F. S., Al Md Ismail, and F. A. Abdullah. "The Implicit Keller Box method for the one dimensional time fractional diffusion equation." *Journal of Applied Mathematics and Bioinformatics* 2, no. 3 (2012): 69-84.
- [16] Osman, S. A., and Trevor Ashley Mcpherson Langlands. "An implicit Keller Box numerical scheme for the solution of fractional subdiffusion equations." *Applied Mathematics and Computation* 348 (2019): 609-626. <https://doi.org/10.1016/j.amc.2018.12.015>
- [17] Habib, Danial, Nadeem Salamat, Sajjad Hussain, Bagh Ali, and Sohaib Abdal. "Significance of Stephen blowing and Lorentz force on dynamics of Prandtl nanofluid via Keller box approach." *International Communications in Heat and Mass Transfer* 128 (2021): 105599. <https://doi.org/10.1016/j.icheatmasstransfer.2021.105599>